Huber et al., http://www.jcb.org/cgi/content/full/jcb.201305076/DC1

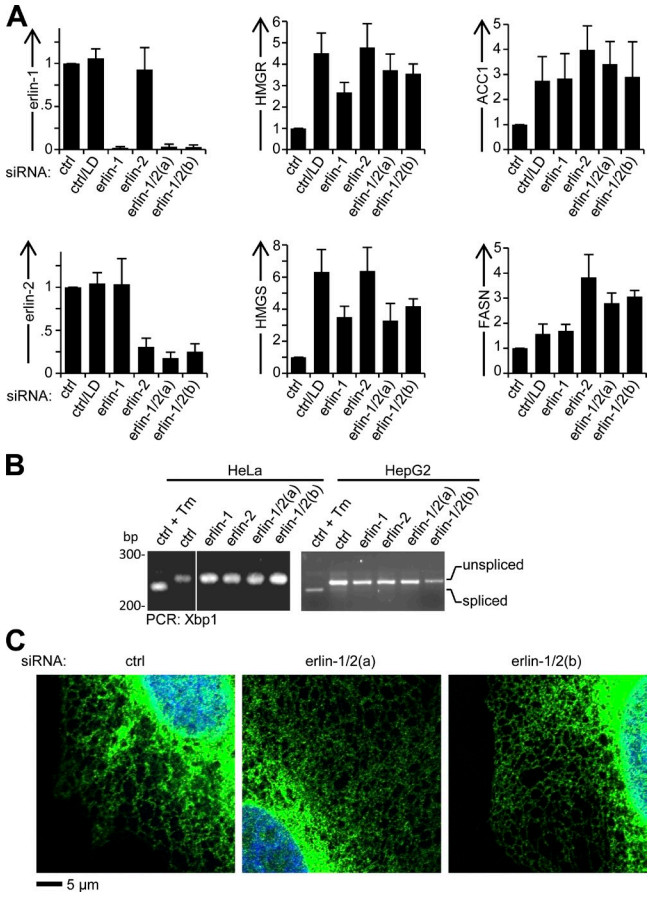

Figure S1. **SREBP target gene activation, UPR status, and ER morphology in erlin-depleted HepG2 and/or HeLa cells.** (A) Erlin silencing and activation of SREBP target genes in HepG2 cells. Levels of the indicated transcripts were determined by q-RT-PCR, in cells treated with nontargeting control (ctrl) or the specified erlin-targeting siRNAs as in Fig. 1 A. P-values for all comparisons with siRNA control <0.006; $n = 4$. Error bars indicate standard deviations. (B) Status of the UPR in erlin-silenced cells. HeLa and HepG2 cells were evaluated by RT-PCR to detect XBP1 splicing. A tunicamycin-treated control for UPR activation is in the first lane. The white line in the gel image (left) indicates where an irrelevant lane was removed for presentation purposes. (C) ER morphology in erlin-silenced cells. HeLa cells, transfected with the indicated siRNAs and an expression construct for Sec61-GFP, were labeled with Hoechst 33342 and visualized by live-cell confocal fluorescence microscopy. The typical tubuloreticular ER pattern is seen in all cases.

THE JOURNAL OF CELL BIOLOGY

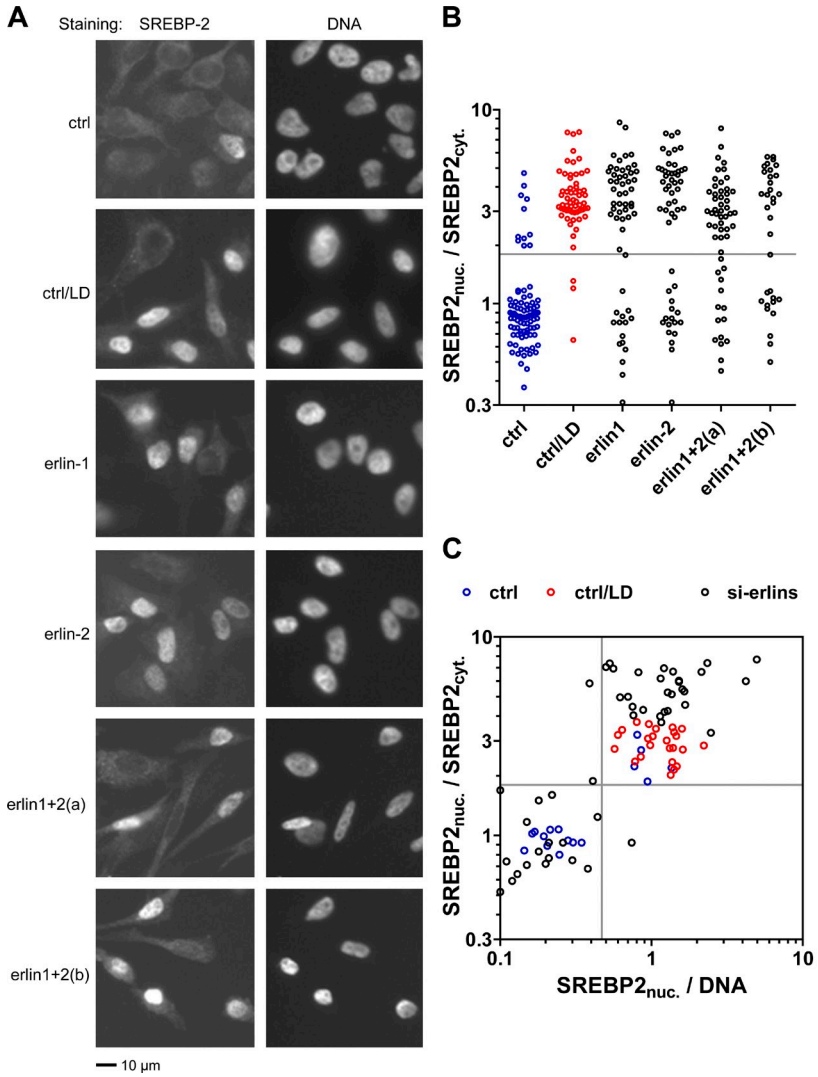

Figure S2. **Accumulation of SREPB-2 in the nucleus of HeLa cells with erlin silencing.** (A) Cells were transfected with control (ctrl) or erlin targeting siRNAs as in Fig. 1 A. Cells were fixed, labeled with an antibody recognizing the N-terminal transcription factor region of SREBP-2, stained with the DNA dye Hoechst 33342, and imaged by fluorescence microscopy in the red (SREBP-2; left) and blue (DNA; right) fluorescent channels. Representative images are shown. Few of the control cells grown under cholesterol sufficiency (ctrl) showed nuclear SREBP-2, whereas almost all control cells in cholesterol depletion conditions (ctrl/LD) displayed strong accumulation of SREBP-2 in the nucleus. Similarly, the majority of the cells in erlin-depleted cultures grown under cholesterol sufficiency showed strong nuclear staining of SREBP-2. (B) Scatter plot of SREBP-$2_{nuc.}$/SREBP-$2_{cyt.}$ ratios in control and erlin-depleted cells. In each category, two to three images from two independent experiments were analyzed. The horizontal line indicates the average of all control (blue circles) and control/LD (red circles) cells and was used as a cutoff to identify SREBP-2–activated cells in Fig. 1 B. (C) Correlation of nuclear SREBP-2 concentration (SREBP-$2_{nuc.}$/DNA) with the nuclear/cytoplasmic ratio of SREBP-2 (SREBP-$2_{nuc.}$/SREBP-$2_{cyt.}$). To test if changes in the nuclear/cytoplasmic ratio of SREBP-2 reflect bona fide changes in the nuclear concentration of SREBP-2, SREBP-$2_{nuc.}$/SREBP-$2_{cyt.}$ was plotted against SREBP-$2_{nuc.}$/DNA. At least three images from two separate experiments (17–33 cells total) were analyzed. Cutoff values differentiating "low" and "high" signals on each ordinate were defined as the average value of control and control/LD samples, and are shown as horizontal and vertical lines within the graph. Cells with low nuclear SREBP-2 generally showed a low SREBP-2 nuclear/cytoplasmic ratio, and cells with high nuclear SREBP-2 showed a high SREBP-2 nuclear/cytoplasmic ratio. Pearson correlation indicated highly significant positive covariance between the two parameters ($r^2 = 0.42$; $P < 0.0001$). Furthermore, most cells with control siRNA in FBS (ctrl; blue) were found in the bottom left quadrant with low SREBP-2, and most lipid-depleted control cells (ctrl/LD; red) were found in the top right quadrant with high SREBP-2, validating the use of nuclear/cytoplasmic ratios as a readout for SREBP-2 and activation in this assay.

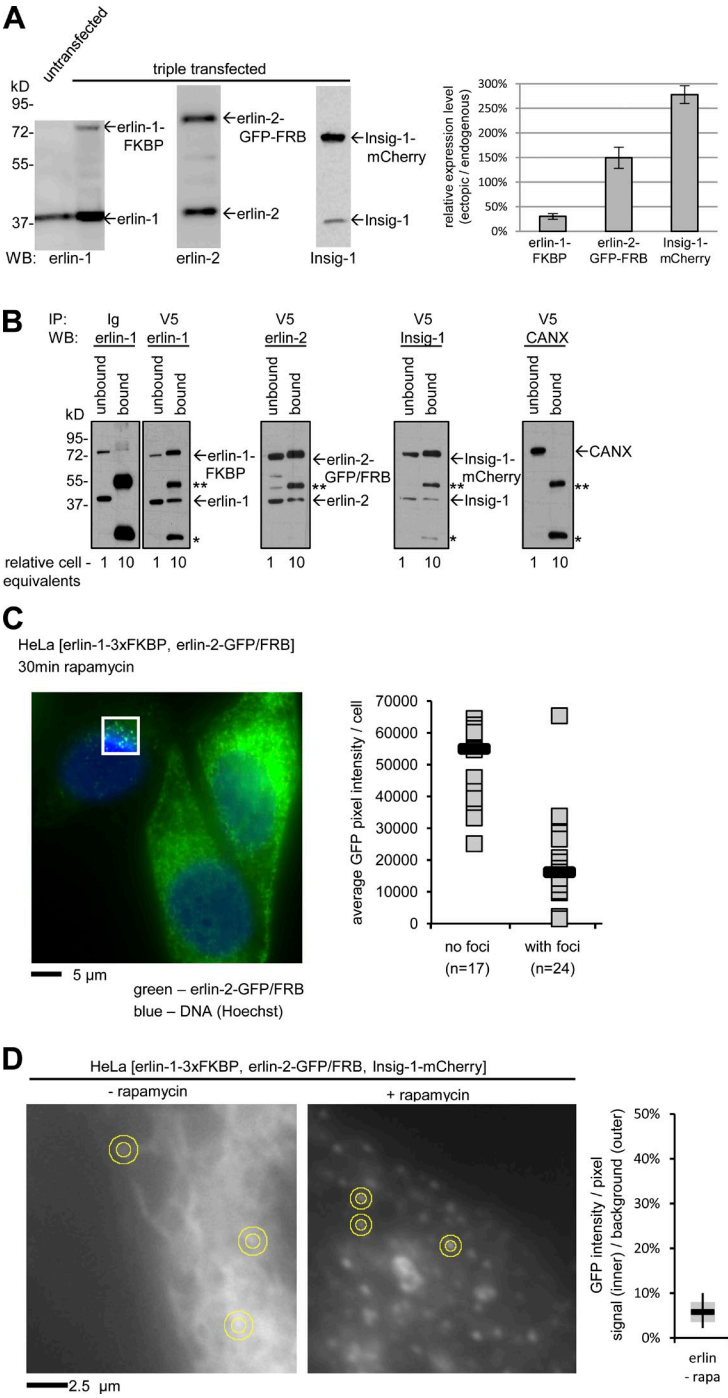

Figure S3. **Biochemical and microscopic characterization of the rapamycin-inducible erlin/Insig-1 clustering system.** (A) Relative expression levels of ectopic versus endogenous erlin-1, erlin-2, and Insig-1 under transfection conditions used for microscopy experiments. HeLa cells were left untransfected (left, first lane) or were cotransfected with DNA constructs encoding erlin-1-FKBP, erlin-2-GFP-FRB, and Insig-1-mCherry ("triple transfected"). Proteins were resolved by SDS-PAGE and detected by Western blotting. Representative gel images are shown on top. Quantitative results, adjusted for transfection efficiency (defined by percentage of GFP-positive cells), are summarized in the bar graph (right; n = 3; error bars indicate standard deviations). (B) Associations between ectopic erlins/Insig and endogenous erlins/Insig assayed by IP. HeLa cells were cotransfected with DNA constructs encoding erlin-1-FKBP-V5, erlin-2-GFP-FRP, and Insig-1-mCherry. Ectopic erlin-1-FKBP-V5 was IPed from cell lysates with V5 antibody (V5). A control reaction with nonspecific IgG is shown in the leftmost panel (Ig). Unbound and bound fractions were analyzed by Western blotting (WB) with antibodies against erlin-1, erlin-2, Insig-1, and calnexin (CANX) detecting endogenous and, where applicable, recombinant forms of these proteins. Cross-reactive signals from IgG heavy and light chains are marked by double and single asterisks, respectively. Relative cell equivalents loaded in each lane are indicated. (C) Relation of erlin-2-GFP-FRB expression level and erlin focus formation. Cells were cotransfected with constructs for erlin-1-FKBP, erlin-2-GFP-FRB, and Insig-1-mCherry, treated with rapamycin, and imaged by wide-field microscopy. Cells containing four to six or more conspicuous foci of concentrated fluorescence were scored as cells with foci (e.g., left panel, leftmost cell; brightness digitally enhanced inside the outlined box). Cells in which the fluorescence largely or completely resembled an ER-like pattern were designated cells without foci (e.g., left panel, two cells on right). Correlation between the level of GFP expression and the designation as cells with or without foci is summarized in the scatter plot (right; gray boxes, individual cells; black horizontal bar, median). 18–24 cells from at least three images of two independent experiments were analyzed. Most cells with foci were in the lower 50th percentile of erlin-2-GFP-FRB–expressing cells. (D) Quantitative image analysis demonstrating that rapamycin-induced erlin-2-GFP-FRB and Insig-mCherry foci are distinct from local intensity fluctuations in the ER. (left) Typical appearance of the GFP signal in cells cotransfected with erlin-1-FKBP, erlin-2-GFP-FRB, and Insig-1-mCherry before the addition of rapamycin. (right) Example of a cell with pronounced GFP foci after the addition of rapamycin. To evaluate the intensity of rapamycin-induced GFP/mCherry foci relative to surrounding background, and to compare these differences to local fluorescence intensity fluctuations that occur in untreated cells, we demarcated 3–6-pixel-diameter circular ROIs (yellow inner circle) containing bright fluorescence. Local background intensity was determined from the 3–4-pixel-wide concentric ring surrounding the original ROI. Three examples are shown in each image. Values for GFP and mCherry staining are summarized in the plot (right; black horizontal bar, average; gray box, SD; black line, range of values), and the average pixel intensity within a focus is expressed as percentage above background. Rapamycin-treated erlin-2-GFP-FRB foci contained substantially higher fluorescence signal above local background than bright ER regions of untreated cells (erlin − rapa vs. erlin + rapa; n = 48 foci in six images from two experiments). Moreover, Insig-1-mCherry foci that appeared in these cells (Insig + rapa) also showed considerably elevated signal over local background. In contrast, local intensity peaks of CANX-mCherry in rapamycin-treated, triple transfected cells were only slightly elevated above local background, similar to erlin-2-GFP-FRB in untreated cells.